T. Jaglinski
Materials Science Program,
University of Wisconsin-Madison,
147 Engineering Research Building,
1500 Engineering Drive,
Madison, WI 53706-1687
e-mail: tmjaglinski@engr.wisc.edu

A. Nimityongskul
Engineering Mechanics Program,
University of Wisconsin-Madison,
147 Engineering Research Building,
1500 Engineering Drive,
Madison, WI 53706-1687
e-mail: apnimityongs@engr.wisc.edu

R. Schmitz
Engineering Mechanics Program,
University of Wisconsin-Madison,
147 Engineering Research Building,
1500 Engineering Drive,
Madison, WI 53706-1687
e-mail: robert.schmitz@ata-e.com

R. S. Lakes
Department of Engineering Physics,
Biomedical Engineering Department,
Rheology Research Center,
University of Wisconsin-Madison,
147 Engineering Research Building,
1500 Engineering Drive,
Madison, WI 53706-1687
e-mail: lakes@engr.wisc.edu

Study of Bolt Load Loss in Bolted Aluminum Joints

Bolted joints are used widely in mechanical design and represent a weak link in a system where loss of joint clamping force can lead to degraded product performance or human injury. To meet current market demands, designers require reliable material data and analysis tools for their industry specific materials. The viscoelastic response of bolted aluminum joints used in the small die-cast engine industry at elevated temperatures was studied. Bolt load-loss tests were performed using strain gages in situ. It was found that after a week at temperature, most bolts lost 100% of their initial prestress. Nonlinear constitutive equations utilizing parameters obtained from uniaxial creep and relaxation tests were used in a simple one-dimensional model to predict the bolt load loss. The model cannot predict the detailed response and overpredicts retained bolt stress for bolt holes that are not preconditioned. For preconditioned holes, the behavior is intermediate between creep and relaxation. [DOI: 10.1115/1.2400262]

1 Introduction

Many technological applications rely on bolted connections to connect components composed of dissimilar materials or complicated geometries as well as providing a means of access and maintenance. Although necessary, these connections provide a weak link where loss of joint clamp force can lead to degraded performance or serious injury in extreme temperature applications. Bolt load loss arises from the time- and temperature-dependent nature of all materials, and in the case of bolted joints, time dependency is manifested by creep or stress relaxation of the structural components.

Die-cast aluminum engine blocks are not immune to time-dependent problems. Small die-cast engines that rely on air cooling can experience transient operating temperatures in excess of half the homologous melting temperature (T_m), where time-dependent behavior is greatly accelerated. High-temperature areas in an engine block include exhaust ports, combustion chambers, and head joints. Loose joints in any of these areas can lead to inefficient operation, escalated emission of pollutants or premature failure. Today's domestic markets, coupled with increasing global product competition, demand low-cost products with long life cycles, where little or no consumer maintenance is required to preserve performance over the product's lifetime. To meet these design goals, detailed knowledge of industry specific material and structural responses is required.

Viscoelastic material behavior, in which we include all time-dependent behavior (i.e., anelasticity or any other form of time-dependent inelastic behavior) can be obtained from uniaxial creep or stress relaxation tests. It would be advantageous to utilize the acquired material parameters from these tests to predict the response of geometrically complex structures subjected to prolonged load and varying time-temperature histories. However, proper use of time-dependent constitutive equations entails an understanding of the detailed stress or strain history to which the structural element is subjected, which can be extremely complex, and the associated boundary conditions, which are heterogeneous in real structures. The actual relaxation behavior of a bolted joint differs from the observed response from a strictly defined creep or relaxation situation. In linear viscoelasticity, creep and relaxation are defined as a material's time-dependent response due to a step input stress or strain, respectively. Furthermore, it is assumed that the boundary conditions remain the same throughout the time period of the step input condition. For a real bolted joint, neither the applied stresses nor strains are step functions due to fluctuating time-temperature histories as well as a partitioning of load between the bolt and flange. For small engines the period of operation is generally short and dominated by a pronounced thermal transient. Such a situation presents challenges for analysis since metals at elevated temperatures are nonlinearly viscoelastic, meaning the time-dependent behavior depends on the applied stress or strain.

The majority of literature concerning experimental time-dependent bolted joint behavior is concerned with steam applications [1] and bridges [2–4]. Most of these studies concern steels of varying compositions [5–8] and some refractory metals [9,10]. Besides aluminum alloys [11], the automotive industry has studied

Contributed by the Materials Division of ASME for publication in the JOURNAL OF ENGINEERING MATERIALS AND TECHNOLOGY. Manuscript received April 28, 2005; final manuscript received May 2, 2006. Review conducted by Matthew P. Millar.

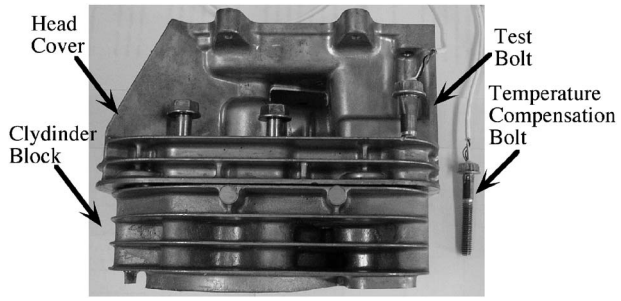

Fig. 1 Example of the die-cast engine head joint studied. This geometry was typical of the eutectic Al–Si alloy head joint.

magnesium alloys [12,13] as well as a phenolic composite [14]. Dynamic properties of bolted joints have also been studied [15]. Many of these experiments have generally been conducted on flange assemblies where the all the components are composed of the same high-temperature material and involve gaskets and nuts. The die-cast engine differs in that the block is composed of one of a series of aluminum-silicon alloys, which are known to exhibit poor high-temperature and creep properties, and use steel fastening bolts, which generally screw into aluminum threads.

To explore the high-temperature, viscoelastic response of the aluminum joints, bolt-load loss tests, using strain gages in situ, were performed on small, air-cooled, die-cast engine blocks typically used on lawn mowers. A model developed elsewhere will be applied in an effort to predict the detailed isothermal structural joint response. To describe the creep behavior of these aluminum alloys, this work will make use of creep data derived from uniaxial tension tests and a nonlinear superposition constitutive equation.

2 Materials and Methods

2.1 Experimental Methods. Bolt-load loss tests, monitored on a steel cylinder head bolt, were run on as-received, die-cast aluminum engine blocks. Three blocks were studied and were composed of an eutectic Al–Si alloy (exact composition is proprietary). No gaskets were used. For ease of handling, the cylinder head joint was cut away from the rest of the engine, as shown in Fig. 1; otherwise, no other modifications were made.

Bolts 8 mm dia, typical of those supplied with each specific engine block, were used to measure the bolt load and were prepared in the following manner. First, two 2.49 mm diameter holes were drilled in the bolt head to allow the gage connection wires to pass through without interfering with the rest of the joint. Two electrical resistance strain gages were then mounted on opposite sides of the bolt shank. For the first two tests, Micro Measurements WK-13-250BG-350 gages were used and for the remaining tests, Micro Measurements WK-06-125AD-350/w. The gage type was changed in order to achieve a lower-profile connection, while the gage size and thermal expansion coefficient were modified to better accommodate the size and material of the bolts.

Teflon® coated connection wires were passed through the bolt head and held in place using CC High Temperature Cement (Omega Engineering Inc.). Once the cement was dry, the wires were connected to the strain gage leads, or solder dots, using a high-temperature solder (570-28R, Micro Measurements Inc.). In addition to placing a small piece of Kapton film (Micro Measurements Inc.) under the soldered connection, another piece of Kapton film was wrapped twice around the outside of the connection to prevent any electrical contact with the cylinder head when the bolt was in place. A dummy temperature compensation bolt was prepared in the same manner. Once the bolts were gaged, the clearance of the bolt shank to the engine holes was reduced from 1.5 mm to 0.5 mm.

Before running tests, the full bridge strain-gage circuit (with two active gages on the loaded bolt and two gages on the dummy temperature compensation bolt) was balanced and shunt calibrated; the bolt was then tightened into the joint. Since applied torque is not directly related to preload due to varying friction losses in each hole, it is paramount that applied bolt strains match for subsequent tests at different temperatures. Thus, bolts were tightened until the appropriate load was achieved by monitoring the strain output. Additionally, two slightly different methodologies were used. First, to mimic manufacturing conditions some holes were not preconditioned in anyway, the bolt was tightened once into the hole. Second, some holes were preconditioned by multiple uses and by tightening the bolt to the desired prestrain, allowing to sit at room temperature overnight and then retightened as necessary.

After tightening the active bolts into place, the dummy bolt for temperature compensation was set into a bolt hole next to the bolt being tightened so that only a portion of the bolt shank was visible. A piece of mineral wool was then wrapped over both bolts to be sure aluminum temperature and not air temperature were being measured. During this time, the test oven was preheated to the desired temperature and allowed to reach steady state before placing the entire gaged head joint into the oven. A Tektronix TDS 420A oscilloscope was used to record strain for the first hour. Data for longer periods of time were taken using the TDS 420A's external clock and a separate function generator as an external trigger.

After a week, the joints were removed from the oven and allowed to cool to room temperature while the strain and temperature were monitored.

Resonant ultrasound spectroscopy (RUS) [16,17] was used to verify the elastic modulus of the bolts being used for these tests. The shank of a bolt was cut to create a steel cylinder with its height equal to its diameter. The cylinder was placed between two shear transducers, such that the edges of the cylinder were in contact with the transducers, and the cylinder was aligned with the BNC cable connector, hence, the direction of shear. One of the transducers was driven with a function generator (Stanford Research Systems, model DS345) and the other was connected to a Tektronix digital TDS 420A oscilloscope. The input frequency was adjusted until the natural frequency was discovered. Using the lowest natural frequency f of the specimen along with Eqs. (1) and (2) the shear modulus was determined.

$$f = \frac{1}{2L}\sqrt{\frac{G}{\rho}} \tag{1}$$

in which L is the cylinder height, ρ is its density, and G is the shear modulus. With

$$E = 2G(1 + \nu) \tag{2}$$

in which the Poisson's ratio ν is 0.33, the elastic modulus E_b was calculated to be 205 GPa.

For RUS, and ultrasonics in general, exact analytical solutions exist to directly obtain Young's modulus and the shear modulus from the natural resonant frequency for specific specimen geometries. For Young's modulus using longitudinal waves, the rod is required to be slender, having a length much longer than the diameter, as well as a diameter much less than the wavelength corresponding to the test frequency. As this was not the case for the bolt geometry that we used, longitudinal measurements would actually reveal a component of the elastic stiffness tensor, and not E. Therefore, it was expedient to measure the shear modulus and use the elastic relationship to obtain E (using Poisson's ratio for steel, which is well known).

2.2 Theoretical Methods. Several investigators have attempted to create analytical models [4,11,14,18] or undertaken finite element analysis (FEA) [8,19] utilizing uniaxial data creep data to model the load-relaxation behavior of bolted joints. These models simply utilize a linear elastic analysis relating measured

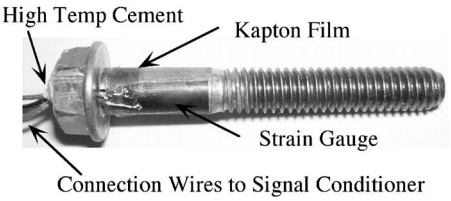

Fig. 2 Typical test bolt and gage assembly

bolt load to the applied preload, thermal loading, and elastic structural compliances of the joint components. Time dependence of the elastic modulus of one or more of the components is described by a phenomenological description of material behavior.

The time-dependent bolt force equation developed by Arimond [14], similar to work by others [4,10,11], was used in this study to predict bolt load loss in a bolted joint and is shown as Eq. (3). This model does not predict bolt load for any general time-temperature history nor does it predict the maximum bolt load from differential thermal expansion of the flange and fastener materials. Thus, Eq. (3) was used only to model bolt load loss after obtainment of the peak thermally induced load. In this analysis, it is assumed the steel bolt is linear elastic

$$F(t) = F_o \frac{C^b + C_o^{al}}{C^b + C^{al}(t)} \tag{3}$$

where, F_o is the initial bolt preload, which will be the maximum observed bolt load after the engine head is brought to operating temperature, C^b is the structural compliance of the bolt, C_o^{al} is the initial aluminum flange compliance, and $C^{\mathrm{al}}(t)$ is the time-dependent aluminum flange compliance. Elastic structural compliances C^b and C_o^{al} are simply the inverse of the standard geometric and material stiffnesses for the elastic elongation of a rod and are calculated using Eqs. (4) and (5). For $C^{\mathrm{al}}(t)$, the structural compliance is calculated the same way as C_o^{al} except Young's modulus E, is replaced by the time-dependent relaxation modulus, $E(t,\varepsilon)$, or the inverse of the creep compliance, $1/J(t,\sigma)$, of the flange material. The relaxation modulus and creep compliance were obtained from uniaxial testing of the flange material, the formulation of $E(t,\varepsilon)$ and $J(t,\sigma)$ are outlined below

$$C = \frac{\lambda}{EA} \tag{4}$$

where E is Young's modulus for each material in question, A is the effective area for the bolt or the flange material, and λ is the thickness of the joint. For this model, λ is assumed to be the length from the base of the bolt head to the third engaged thread of the bolt [19]. The analytical model was also run using the entire bolt length, and the models after one week at operating temperature had $<2\%$ difference as compared to the shorter assumed length model. The effective area for the flange can be approximated as a frustum of a cone and is shown as [20]

$$A_c = \frac{\pi}{4}(d_{bh}^2 - d_h^2) + \frac{\pi}{8}\left(\frac{d_j}{d_{bh}} - 1\right)\left(\frac{d_{bh}\lambda}{5} + \frac{\lambda^2}{100}\right) \tag{5}$$

where A_c is the equivalent area, d_{bh} is the diameter of the bolt head, d_h is the diameter of the hole, and d_j is the length from the edge of the hole to the edge of the flange material. We note that a similar equation is presented in Ref. [4]; however, the first term in their Eq. (5) has been presented as a sum when it should be a subtraction of the hole area.

Prior to this study, uniaxial creep and relaxation tests were performed on the same alloys previously discussed in this work. Jaglinski and Lakes [21] showed that the eutectic Al–Si alloy exhibited nonlinear viscoelastic behavior for temperatures ranging between 220°C and 280°C. The creep in this regime was primary creep. Using the data collected over a range of stress and temperature, nonlinear constitutive equations were developed following the technique outlined by Oza et al. [22] Though these equations phenomenologically describe the material response, these formulations can be used to describe the stress dependence of the creep compliance, provide an avenue for interrelation between creep and relaxation, and allow extrapolation between creep/relaxation curves so only limited mechanical testing is required. Furthermore, these formulations are not restricted to metals but can be applied to other weakly nonlinear materials.

Nonlinearity in time-dependent behavior may be developed from the bottom up, beginning with linear viscoelasticity and incorporating progressively more nonlinearity, using single integral or multiple integral constitutive formulations. That approach, common in the context of polymers and biological materials, is appropriate if the nonlinearity is relatively weak, as is the case for the present results. Conversely, one may begin with plasticity, which is inherently nonlinear (with a threshold stress), and then incorporate time dependence. Theories of time-dependent plasticity are referred to as viscoplasticity [23], and those that involve the notion of damage are called damage mechanics models [24]. Viscoplasticity models are available that do not involve any threshold [25]. Such a viscoplastic approach could be used to model the present experimental results; we do not claim the approach used is unique. Recovery experiments were not conducted on the present material; thus, it is not known whether the applied strains and stresses applied experimentally induced permanent deformation.

The assumed two-term form for the stress-dependent creep compliance, $J(t,\sigma)$, is shown as Eq. (6); more terms can be used if a higher degree of nonlinearity needs to be accommodated. $J(t,\sigma)$ is formulated from a three-point isochronal method constructed from experimental uniaxial creep curves for each specific alloy. An isochronal is a stress-strain plot for several points in stress, where the applied stresses are chosen at identical times for the different creep curves. Several creep curves at varying levels of stress, but constant temperature, are required for the construction. Thus, a separate $J(t,\sigma)$ is required for each operating temperature

$$J(t,\sigma) = g_1 + g_2\sigma^p t^n \tag{6}$$

Here, material parameters g_1, g_2 and time exponent n are acquired from the isochronal method. p is the stress exponent and has been chosen to be 0.75 because this value fits well with the isochronal data points of the metals [8]. Here, the units for time t are seconds and for stress σ are Pa.

Briefly, isochronals are constructed as follows. For the two-term expression of Eq. (6), two empirical creep curves at different levels of applied stress but at constant material composition and temperature are required. Three steps are required to find the values of g_1, g_2, and n, and thus three isochronal points are required at time $t=0,1$ and any other point in time ($t=x$). (i) The isochronal for $t=0$ is used to obtain g_1, (ii) the isochronal for $t=1$ and g_1 are used to obtain g_2, and (iii) the isochronal for $t=x$ and the values of g_1 and g_2 are used to obtain n. For this analysis, strains at three times, $t=10$, 5×10^3, 1×10^5 s were used. In the most general application of the method, $t=0$ is required to obtain the first term in Eq. (6). However, the actual creep test has no time zero due to a $\sim$2 s rise time in the creep frame; the applied load is not a true step function. Since data were not reported until 10 s into the creep test, the time variable must be shifted according to the details given by [22] to account for this. The final functional form of $J(t,\sigma)$ used for the analysis is shown in Eq. (7), and the creep strain can be calculated using Eq. (8).

$$J(t,\sigma) = g_1 + g_2\sigma^{0.75}\left(\frac{t-10}{4990}\right)^n \tag{7}$$

$$\varepsilon(t) = J(t,\sigma)\sigma \tag{8}$$

Table 1 Dimensional data and material parameters. Units for g_1 are Pascal to the −1 and f_1 are Pascal.

Dimensions	Temp.	g_1	g_2	n
$\lambda=0.036$ (m)	220°C	1.478×10^{-11}	1.094×10^{-18}	0.485
$d_b=0.008$ (m)	240°C	1.510×10^{-11}	6.050×10^{-18}	0.280
$d_{bh}=0.0165$ (m)	260°C	1.503×10^{-11}	6.139×10^{-18}	0.340
$d_h=0.095$ (m)		f_1	f_2	n
$d_j=0.005$ (m)	220°C	7.53×10^{10}	-1.36×10^{12}	0.246
$A_b=5.02\times10^{-5}$ (m^2)	240°C	7.16×10^{10}	-1.27×10^{12}	0.2942
$A_c=1.07\times10^{-4}$ (m^2)	260°C	7.17×10^{10}	-1.39×10^{12}	0.3139

Relaxation is modeled in a similar manner as that used for creep; however, if no relaxation data are available, an alternate route is to use the interrelationship between creep and relaxation to obtain the relaxation modulus from the creep compliance equation [26]. Here we obtain the relaxation modulus, $E(t,\varepsilon)$ from isochronals constructed from relaxation data, with the functional form shown as

$$E(t,\varepsilon)=f_1+f_2\varepsilon^{0.75}\left(\frac{t-10}{4990}\right)^n \tag{9}$$

and the relaxation stress as

$$\sigma(t)=E(t,\varepsilon)\varepsilon \tag{10}$$

where f_1, f_2, and n are empirical material constants and ε is the applied strain.

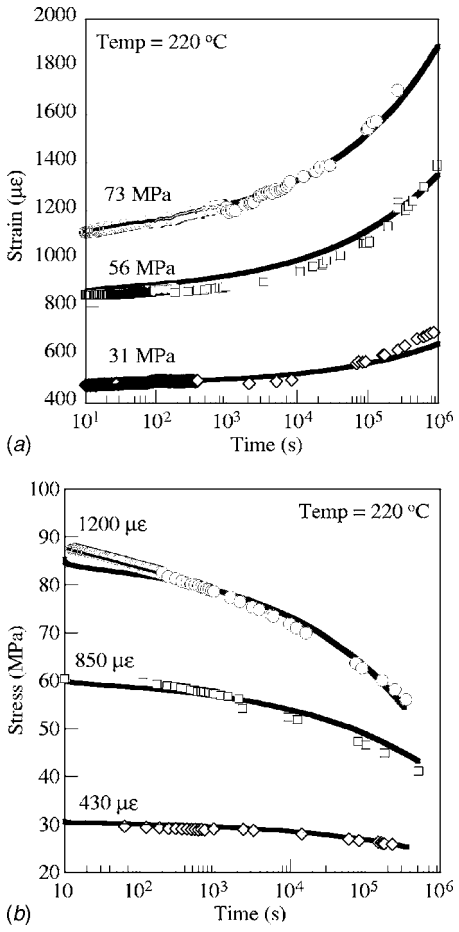

Fig. 3 Comparison between nonlinear superposition model (solid lines) and uniaxial data (open point shapes) for (*a*) creep at several stresses and (*b*) relaxation at several strains, were both are at a temperature of 220°C.

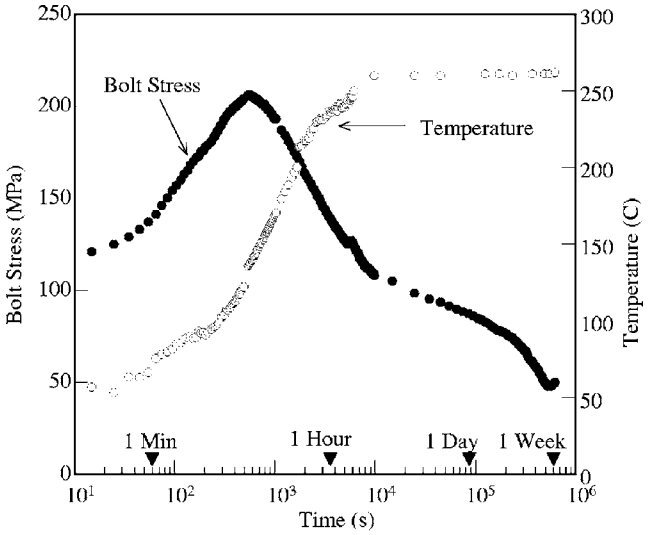

Fig. 4 Typical thermal response for the bolted joints tested in this study. Steady-state temperatures are not achieved until 1–2 h into a given test. Note the time reference labels, which will be included without text in subsequent figures.

Table 1 includes all the data used for the analysis. Since $n<1$, all the creep is primary creep.

To illustrate the ability of the formulations to model the data, the predictions for creep and relaxation at a temperature of 220°C, as shown in Fig. 3. The curves presented use the functional forms and the material parameters obtained from uniaxial constant load creep and stress relaxation experiments done in tension.

3 Results

3.1 Observed Bolt Load Loss. Room-temperature relaxation was monitored for all bolted joint tests. It was found that even at room temperature, where viscoelastic deformation should be minimal, the bolts experienced some load loss, which is attributed to embedment relaxation. Embedment relaxation is defined as localized plastic deformation due to small material imperfections on thread contact surfaces [6,20]. Bickford [20] suggests an initial 10% loss from embedment relaxation, which is consistent with the observed results. Most of the preload loss due to embedment was experienced within the first few minutes after tightening.

With the assumed stressed area of the aluminum from Eq. (5), the initial prestrain applied to the bolts corresponds to roughly 25% of the aluminum alloy's room-temperature yield strength. At highest testing temperature of 260°C, the initial preload corresponds to 50% of the yield strength in the aluminum alloy.

Figure 4 shows the typical thermally induced bolt load response as the joint is heated, with these particular data from the first tested flange. Steady-state temperature was not reached until 1–2 h had elapsed for a given test. Time to thermal equilibrium depended on each particular joint geometry because each varied in total mass. Note, the kink in the experimental stress data presented in Fig. 4, is due to a change in strain gage conditioner channels, necessitated by the onset of a problem in the first channel used.

Figure 5 shows all tests conducted on the first joint at three different temperatures with some variability in the prestresses. These bolts were tightened once into unused holes and placed into the oven. The transient temperature data have not been included because the increase in temperature followed a similar pattern as that shown in Fig. 4, reaching a steady-state temperature after about 1–2 h into the test. The three tests were run on temperatures of 220 (◇), 240 (△) and 260°C (●). The detailed response

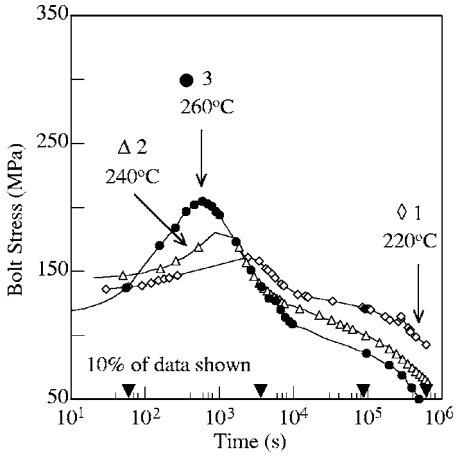

Fig. 5 Measured bolt stress for all tests from the first flange for three temperatures; the joint did not reach thermal equilibrium until 1–2 h after placement into the preheated furnace. All tests were run in unused holes.

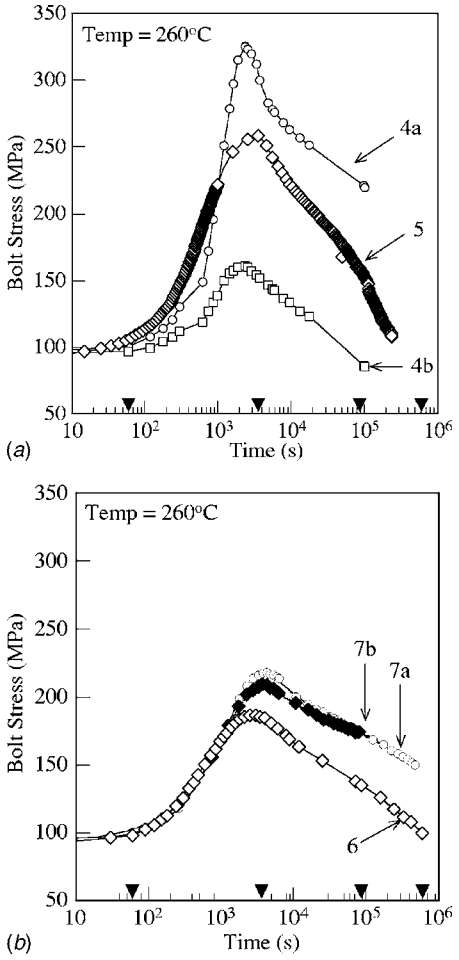

Fig. 6 Measured bolt stress for the second block tested at 260°C showing (*a*) three tests using the manufacturing method in unused holes and (*b*) three tests run in preconditioned holes. Tests marked a and b were run concurrently (in different holes). Test 7b lost electrical contact before one week had elapsed.

of this joint showed the expected thermally induced load; however, a change in the relaxation slope after reaching thermal equilibrium was observed but is not seen in uniaxial testing. After a week, the bolts exposed to 240°C and 260°C lost all prestress with the bolt exposed to 220°C, retaining only ~20% of the original prestress.

Figure 6 shows data acquired from the second block, which was only tested at 260°C. Figure 6(*a*) shows data from three bolts which were tightened once in untested holes and placed in the oven. For the second block, the curves marked 4a and 4b represent two separate bolts tested concurrently. As can be seen, the thermally induced loads vary substantially between tests. A second series of tests was run in the previously used holes and are shown in Fig. 6(*b*). Again, tests marked 7a and 7b were separate bolts run concurrently. After the preconditioning, the thermally induced loads seem to be more consistent. The electrical connection for test 7b was lost before the completion of the experiment hence the curve is truncated.

The third block was tested at 240°C and 220°C, with all tests except for the initial (test 8 in Fig. 7) done in preconditioned holes. Again, tests marked a and b were run concurrently. Except for the initial test 8, the thermally induced loads are fairly consistent between tests.

Figure 8 shows a comparison between the bolt load response of the preconditioned holes for the second and third blocks. As expected, bolts exposed to higher temperatures experienced a higher thermally induced load and relaxed faster than bolts tightened to the same initial prestress but exposed to lower temperatures. Predictions based on elastic thermal expansion give rise to a considerable overestimate of maximum load. The thermally induced load prediction for the 260°C test was 16% higher than the response seen from the preconditioned holes. Likewise, the predictions for the 240°C and 220°C tests overpredicted the response by 22% and 23%, respectively. This is expected because the viscoelastic response must be considered at elevated temperature, especially as the induced thermal load is substantial.

After a week at temperature, the joints were removed from the oven while strain and temperature were monitored. An example of the cooldown is shown in Fig. 9 for tests 12 and 13, which were run at 220°C. After a week at elevated temperature, all bolts exposed to temperatures higher than 220°C lost 100% of their original prestress after cooling to room temperature and are not shown. In many cases, these bolts could be removed from the block by hand. Bolts raised to only 220°C retained ~20% or less of their original prestress.

3.2 Analytical Results. Figure 10 shows the theoretical predictions from use of the nonlinear creep compliances and the model of Eq. (3) for the first and second flanges for bolts that were tightened once and placed in the oven. In every case, except test 4a, models based on creep overpredict the retained bolt stress after a week at temperature. Models based on relaxation (dashed lines) show significant deviation from the experiment, shown as an example for test 4a (Fig. 10(*b*)). Furthermore, as expected the simplicity of the model does not predict the detailed behavior of the joint because it does not capture the slope changes. However, for the lower temperatures, the model is within reasonable accuracy at the end of a week. These sudden slope changes do not appear in the uniaxial data. The shape of the load loss curves is not consistent for the two flanges, with the first flange (Fig. 5) showing several pronounced slope changes in all three tests after several hours into each test. Slope changes can be seen in the unconditioned holes for the second flange at 260°C (Fig. 6(*a*)), but no pronounced slope changes were seen in the unconditioned holes.

Figure 11 shows theoretical predictions for the preconditioned holes of the second and third flanges at 260°C and 220°C. Specifically, experiments 7a and 13 are shown. For the preconditioned holes, experimental behavior is intermediate to behavior predicted from relaxation (dashed lines) and creep (thick lines). For the other experiments on preconditioned holes, as well as those at 240°C, which are not shown, data fall between predicted creep and relaxation behavior.

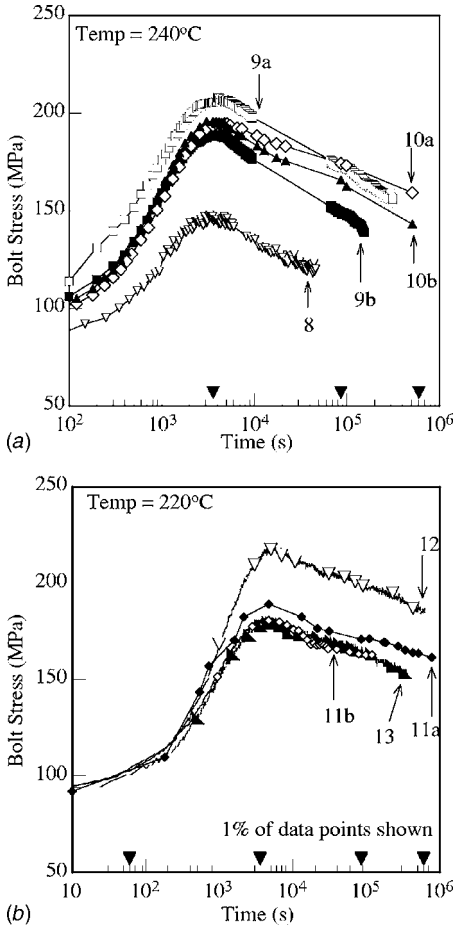

Fig. 7 Measured bolt stress for the third block tested at (a) 240°C and (b) 220°C. All tests except for 8 in (a) were preconditioned. Again, tests marked a and b were run concurrently (in different holes). Note, in (b) the results for tests 11b and 13 lie almost on top of each other.

4 Discussion

The simple analysis undertaken in this study shows that data from uniaxial creep tests can be employed to predict the performance of bolted joints through the use of a nonlinear viscoelastic formulations. Formulations based on creep and relaxation both predict a decrease in bolt load from the peak thermal load as functions of time. For unconditioned holes, models using the creep compliance equation overpredict retained bolt load by an average of ~24%. For conditioned holes, creep models underpredict the retained load by 30% for a temperature of 260°C and only 10% for a temp of 220°C; conversely, relaxation models overpredict retained load by 20% for 260°C and 9% for 220°C.

The results for the preconditioned holes may also answer a question of loose terminology. The terms bolt load relaxation and creep are interchanged arbitrarily in the literature. Observed bolt load does decrease, or relax, with time. However, as previously stated, stress relaxation is defined as a material's time-dependent stress response to a step input strain, which is not the same as creep. The actual governing equation for a particular bolted joint will depend on the ratio between the structural compliances of the bolt and flange material. Extremes of this ratio (i.e., the bolt being much stiffer than the flange or much more compliant than the flange material) will lead to material behavior explicitly following

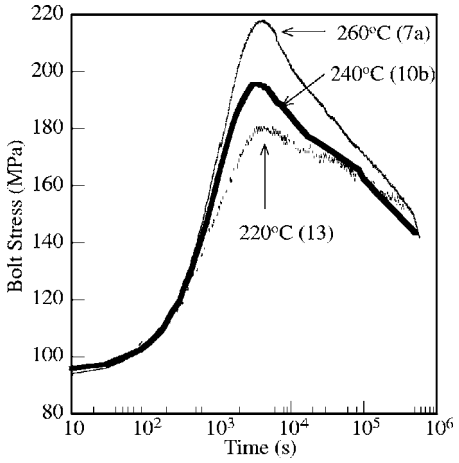

Fig. 8 Comparison of the bolt load response for preconditioned holes from the second and third blocks at three different temperatures. Tests 7a (260°C), 10b (240°C), and 13 (220°C) are shown.

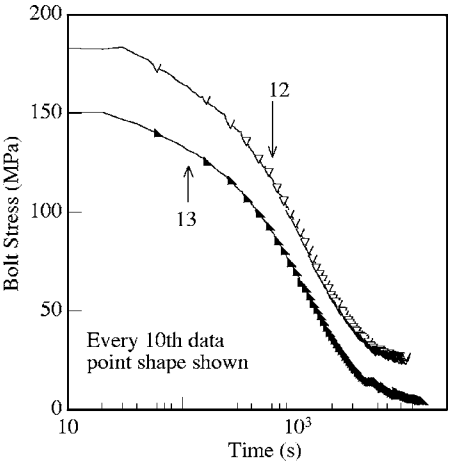

Fig. 9 Representative bolt load response during cool down from 220°C to room temperature for tests 12 and 13, which showed retained bolt load.

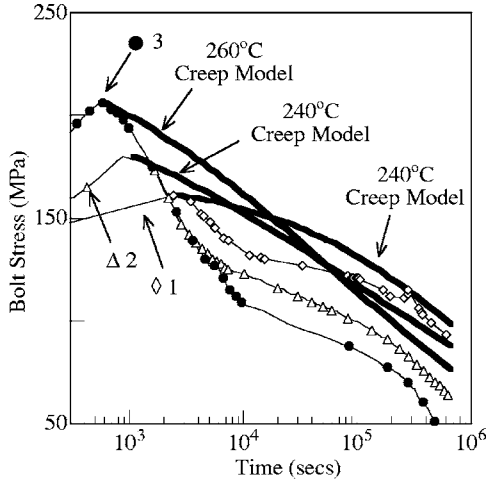

Fig. 10 Theoretical predictions (thick lines) beginning from the peak thermal load as the step input condition for (*a*) the first flange and (*b*) the second flange at 260°C. All tests in this figure were tightened once and placed in the oven. Behavior based on the relaxation formulation (dashed line in (*b*)) significantly deviates from the experiment and is only shown in for test 4a for comparison.

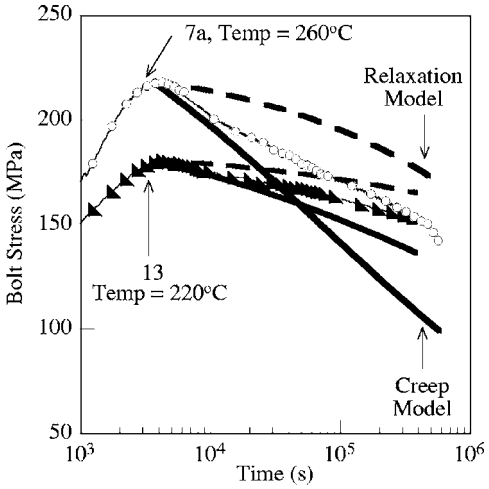

Fig. 11 Theoretical behavior from peak thermal load for preconditioned holes from the second and third flanges for 260°C and 220°C. Experimental behavior lies between behavior based on creep (thick lines) and relaxation (dashed lines); similar behavior is seen for 240°C but is not shown for clarity.

either its relaxation modulus or its creep compliance. For the case studied herein, the ratio of bolt and flange structural compliances is intermediate. In fact, the experimental behavior for conditioned holes is intermediate between behavior predicted from creep and relaxation. Interrelation of creep and relaxation results can be done for linear viscoelastic materials; however, for nonlinear ones the interrelation is considerably more difficult [22,26]. Analytical interrelation for the intermediate case of a bolted joint is not yet available.

Despite the fact that the models used herein predict bolt loss to within 9–30%, it will be expedient to attempt to refine the present technique by capturing more material physics in the basic constitutive equations. Specifically, inclusion of temperature dependence into the present creep compliance formulation will allow the use of a single constitutive equation to model material behavior, either analytically or computationally, subject to any general load or temperature time history. This is especially useful when one considers the operational cycle and lifetime of small die-cast engines

Some other ways in which this model could be improved are (i) construction of the relation between bolt and flange compliances with observed bolt stress directly within the framework of linear viscoelasticity and (ii) consideration of the entire heterogeneous stress state and stress concentrations. The integral formulations that usually result from a linear viscoelastic analysis offer enough flexibility to model a wide range of material behavior. Though the resulting equations can have a high degree of complexity, they can be evaluated numerically. Utilization of FEA analysis to handle the heterogeneous stress state under the head of the bolt and in the aluminum threads may lead to a closer convergence between theory and experiment.

5 Conclusions

It was found that, after a week at temperature and subsequent cooling to room temperature, all bolts tested above 220°C showed 100% loss of prestress, whereas bolts exposed to 220°C retained around 20% of their initial prestress. Bolt load loss curves showed a more complex response than the typical creep or relaxation curve. Nonlinear constitutive equations to describe material behavior, where creep compliance depends on applied stress and relaxation modulus depends on applied strain, in conjunction with a simple structural model can predict joint performance to within 9–30%. For unconditioned holes, creep-based models overpredict retained bolt stress at temperature by an average of 24%. For conditioned holes, the behavior is intermediate between creep and relaxation. Creep-based models in this case underpredict the retained load by 30% for a temperature of 260°C and only 10% for a temperature of 220°C, conversely relaxation models overpredict retained load by 20% for 260°C and 9% for 220°C. Deviations of the model from experiment are attributed to lack of consideration of the actual heterogeneous stress state and not properly accounting for the actual boundary conditions in the joint.

References

[1] Strang, A., ed., 1994, *Performance of Bolting Materials in High Temperature Plant Applications*, Institute of Materials, London.

[2] Sarisley, E. F., and Accorsi, M. L., 1990, "Prestress Level in Stress-Laminated Timber Bridges," Adv. Environ. Res., **116**, pp. 3003–3019.

[3] Tendo, M., Yamada, K., and Shimura, Y., 2001, "Stress Relaxation Behavior at High-Tension Bolted Connections of Stainless-Steel Plates," ASME J. Eng. Mater. Technol., **123**, pp. 198–202.

[4] Yang, J., and DeWolf, J. T., 1999, "Mathematical Model for Relaxation in High-Strength Bolted Connections," Adv. Environ. Res., **125**, pp. 803–809.

[5] Ellis, F. V., and Tordonato, S., 2000, "Calculation of Stress Relaxation Properties for Type Stainless Steel," ASME J. Pressure Vessel Technol., **122**, pp. 66–371.

[6] Kumankura, S., Hosokawa, S., and Sawa, T., 1998, "Bolt Load Reduction of Bolted Joints Under External Axial Load," *Analysis of Bolted Joints*, Hsu, K. H., and Sawa, T., eds., ASME, New York, pp. 103–108.

[7] Kraus, H., and Rosenkrans, W., 1984, "Creep of Bolted Flanged Connections," Weld. Res. Counc. Bull., **294**, pp. 2–8.

[8] Maile, K., and Klenk, A., 1999, "Numerical Analysis of High Temperature Pipe Flanges," *Analysis of Bolted Joints*, Hsu, K. H., and Sawa, T., eds. ASME, New York, pp. 53–160.

[9] Ellis, F. V., Sielski, D. R., and Viswanathan, R., 2001, "An Improved Analytical Method for Life Prediction of Bolting," ASME J. Pressure Vessel Technol., **123**, pp. 70–74.

[10] Roos, E., Xu, H., Klenk, A., and Meile, K., 1999, "Description of Deformation and Failure Behavior of a Nut-Bolt-Assembly by Means of a Viscoplastic Constitutive Equation." *Analysis of Bolted Joints*, Hsu, K. H., and Sawa, T., eds. ASME, New York, pp. 95–102.

[11] Webster, J., 1994, "Design Formula to Predict Retained Steel Bolt Strength When Joining A380 Aluminum Components at High Temperatures," SAE Paper No. 941738.

[12] Chen, F. C., Jones, J. W., McGinn, T. A., Kearns, J. E., Nielsen, A. J., and Allison, J. E., 1997, "Bolt-Load Retention and Creep of Die-Cast Magnesium Alloys," Characteristic and Applications of Magnesium in Automotive Design, SAE International Congress & Exposition, Detroit, pp. 13–21.

[13] Pettersen, K., and Fairchild, S., 1997, "Stress Relaxation in Bolted Joints of Die Cast Magnesium Components," Characteristic and Applications of Magnesium in Automotive Design, SAE International Congress and Exposition, Detroit, pp. 23–31.

[14] Arimond, J., 1997, "Bolt Load Retention Modeling From Creep Performance Data." Advances in Automotive Plastic Components and Technology, SAE International Congress and Exposition, Detroit, pp. 7–11.

[15] Esmailzadeh, E., Chorashi, M., and Ohadi, A. R., 1996, "Analysis of Preloaded Bolted Joints Under Exponentially Decaying Pressure," ASME J. Pressure Vessel Technol., **118**, pp. 393–398.

[16] Lee, T., Lakes, R. S., and Lal, A., 2000, "Resonant Ultrasound Spectroscopy for Measurement of Mechanical Damping: Comparison With Broadband Viscoelastic Spectroscopy," Rev. Sci. Instrum., **71**, pp. 2855–2861.

[17] Wang, Y. C., and Lakes, R. S., 2003, "Resonant Ultrasound Spectroscopy in Shear Mode," Rev. Sci. Instrum., **74**, pp. 1371–1373.

[18] Zerres, H., Perez, M., Lemauviel, L., and Scliffet, L., 1998, "Comparison Between the Analysis of the Mechanical Behavior of Bolted Joints by the Finite Elements Method and by the Eurpean Approach." *Analysis of Bolted Joints*, Hsu, K. H., and Sawa, T., eds., ASME, New York, pp. 69–73.

[19] Cook, R., and Young, W., 1999, *Advanced Mechanics of Materials*, 2nd ed., Prentice-Hall, Englewood Cliffs, NJ.

[20] Bickford, J. H., 1995, *An Introduction to the Design and Behavior of Bolted Joints*, 3rd ed., Marcel Dekker, New York.

[21] Jaglinski, T., and Lakes, R. S., 2004, "Creep Behavior of Al–Si Die-Cast Alloys," ASME J. Eng. Mater. Technol., **126**, pp. 378–382.

[22] Oza, A., Lakes, R. S., and Vanderby, R., 2003, "Interrelation of Creep and Relaxation or Nonlinearly Viscoelastic Materials: Application to Ligament and Metal," Rheol. Acta, **42**, pp. 557–568.

[23] Cristescu, N., and Suliciu, I., 1982, *Viscoplasticity*, Marinus Nijhoff, The Hague.

[24] Schapery, R. A., 1999, "Nonlinera Viscoelastic and Viscoplastic Constitutive Equations With Growing Damage.," Int. J. Fract., **97**, pp. 33–66.

[25] Lubliner, J., 1990, Plasticity Theory, Macmillan, New York.

[26] Lakes, R. S., and Vanderby, R., 1999, "Interrelation of Creep and Relaxation: A Modeling Approach for Ligaments," ASME J. Biomech. Eng., **121**, pp. 612–615.